

Spatial-Temporal Reinforcement Learning for Network Routing with Non-Markovian Traffic*

Molly Wang^{**} and Kin K. Leung[†]

^{**}Department of Computing, Imperial College London, UK

[†]Departments of Electrical & Electronic Engineering, and Computing, Imperial College London, UK

^{**}jw923@imperial.ac.uk, [†]kin.leung@imperial.ac.uk

Abstract—Reinforcement Learning (RL) has become a well-established approach for optimizing packet routing in communication networks. Standard RL algorithms typically are based on the Markov Decision Process (MDP), which assumes that the current state of the environment provides all the necessary information for system evolution and decision-making. However, this Markovian assumption is invalid in many practical scenarios, making the MDP and RL frameworks inadequate to produce the optimal solutions. Additionally, traditional RL algorithms often employ function approximations (e.g., by neural networks) that do not explicitly capture the spatial relationships inherent in environments with complex network topologies. Communication networks are characterized by dynamic traffic patterns and arbitrary numbers of nodes and links, which further complicate the decision-making process. To address these challenges, we propose a spatial-temporal RL approach that integrates Graph Neural Networks (GNNs) and Recurrent Neural Networks (RNNs) to adequately capture the spatial dynamics regarding network topology and temporal traffic patterns, respectively, to enhance routing decisions. Our evaluation demonstrates that the proposed method outperforms and is more robust to changes in the network topology when compared with traditional RL techniques.

I. INTRODUCTION

The rapid growth in network size and traffic volume, driven by social media, video streaming, and 5G, has created new challenges for routing optimization in communication networks such as software-defined networks (SDNs). One significant issue is inter-domain traffic engineering or Wide-Area Network (WAN) optimization, which involves optimizing traffic routing across multiple domains. These problems are often NP-hard, making analytical methods difficult to apply [1]. Traditional machine learning approaches for routing often require labeled data, which may not always be available for large-scale networks [2].

RL provides a model-free approach by learning optimal policies through environment interactions. Deep reinforcement learning (DRL) methods, like Deep Q-Network (DQN), have been applied to communication network routing [3], [4]. While they are effective for discrete actions, they struggle with continuous problems such as bandwidth allocation. Policy gradient methods that can handle continuous action spaces through direct policy optimization can be used to address this challenge [5].

* Kin K. Leung was supported by the Dstl SDS Continuation project and EPSRC grant EP/Y037243/1.

Despite its popularity, traditional RLs often struggle with non-Markovian behaviors of network traffic and fail to consider temporal dynamics in data traffic [6]. Existing solutions have used periodic Markov Decision Processes (pMDPs) to model, for example, the diurnal patterns of cluster trace data [7], but these approaches fall short of capturing more complex non-stationary traffic patterns.

DRL architectures often employ fully connected feed-forward neural networks (FFNNs) for function approximations, but they do not model the spatial relationship in environments with a topology. While convolutional neural networks (CNNs) can capture Euclidean spatial structure (e.g., image-based pixels), they are not suitable for irregular topology.

Motivated to address these issues, this paper presents a Spatial-Temporal Reinforcement Learning (STRL) technique to capture and integrate both spatial and temporal dimensions in communication networks by using Graph Neural Networks (GNNs) and Recurrent Neural Networks (RNNs), respectively. In particular, we apply the STRL approach to determining the optimal network routing. The contributions of this paper are:

- Propose a new STRL approach to capturing complex temporal patterns (e.g., non-stationarity) in communication network traffic by utilizing Gated Recurrent Units (GRUs) with a temporal attention mechanism.
- The new approach also captures spatial relationships using Graph Attention Networks (GATs).
- Demonstrate the importance of jointly considering spatial-temporal dynamics for better routing decisions compared to solely temporal or spatial approaches.
- Reveal the robustness of the proposed method against change of network topology, which is not in the training data.

II. PRELIMINARIES

A. Reinforcement Learning

RL is a machine learning approach where an agent learns to make decisions by interacting with an environment modeled by MDPs. Unlike supervised learning, RL learns from the consequences of its actions by observing and using feedback from the environment. The key components of RL include the agent, the environment, states (S), actions (A), rewards (R), the value function (V), the action-value function (Q), and the policy (π). The environment, modeled as an MDP, is

defined by a tuple $\langle \mathcal{S}, \mathcal{A}, r, \mathcal{P} \rangle$ where \mathcal{S} is the state space, \mathcal{A} is the action space, r is the reward function, and \mathcal{P} is the state transition probability function. In each time step, the agent observes the current state $s \in \mathcal{S}$, takes an action $a \in \mathcal{A}$, and receives a reward r , with the state transitioned to a new state $s' \in \mathcal{S}$ with probability $\mathcal{P}_{ss'}^a = P(s'|s, a)$.

B. Deep Deterministic Policy Gradient (DDPG)

RL algorithms are categorized into value-based methods, which learn a value function representing expected long-term rewards (e.g., Q-learning, DQN), and policy-based methods, which directly learn the policy as a probability distribution over actions for given states (e.g., REINFORCE). To exploit the merits of both approaches, we use DDPG for its off-policy actor-critic framework.

DDPG leverages off-policy learning by using a behavior policy for exploration and optimizing the target policy with experiences stored in a replay buffer [10]. This encourages the exploration of different routing paths without being restricted to the current behavior policy. The actor-critic framework includes two networks: the actor, mapping states to actions, and the critic, estimating the Q -value of these actions, which improves learning stability. As a result, DDPG employs four networks: the behavior actor (μ) and critic (Q), and the target actor ($\hat{\mu}$) and critic (\hat{Q}). The term "deep" reflects the use of deep neural networks to parameterize both actor and critic, with distinct optimization methods.

For the behavior critic network, denoted as Q , we aim to optimize its parameters θ by minimizing the mean squared error loss:

$$L(\theta) = \mathbb{E}[(Q(s, a|\theta) - y)^2], \quad (1)$$

where $Q(s, a|\theta)$ approximates the expected return from state s and action a . The target Q -value, y , is computed using the Bellman equation:

$$y = r + \gamma \hat{Q}(s', \hat{\mu}(s'|\hat{\omega})|\hat{\theta}),$$

where r is the immediate reward, s' is the next state, and \hat{Q} is the target critic network with parameters $\hat{\theta}$. The action $a' = \hat{\mu}(s'|\hat{\omega})$ is chosen by the target actor network $\hat{\mu}$, parameterized by $\hat{\omega}$. The discount factor $\gamma \in [0, 1]$ balances short-term and long-term rewards.

The behavior actor network μ , parameterized by ω , is optimized using the deterministic policy gradient. "Deterministic" implies that for a given state s , the actor produces a specific action $a = \mu(s|\omega)$, rather than a probability distribution (e.g., $a \sim \pi(a|s)$). The actor maximizes the Q -value predicted by the behavior critic network Q to select actions that yield higher long-term rewards. The actor's policy gradient is given by:

$$\nabla_{\omega} J(\mu_{\omega}) \approx \mathbb{E}(\nabla_a Q(s, a|\theta)|_{a=\mu(s)} \nabla_{\omega} \mu(s|\omega)),$$

where $J(\mu_{\omega}) = \mathbb{E}_{s \sim d^{\mu}} [Q(s, \mu_{\omega}(s))]$ is the expected Q -value, with states s distributed as d^{μ} under μ . The term $\nabla_a Q(s, a|\theta)$ indicates how changes in a affect the Q -value, while $\nabla_{\omega} \mu(s|\omega)$ shows how to adjust ω to maximize $Q(s, a)$.

In practice, averaging over a mini-batch approximates the expectation:

$$\nabla_{\omega} J(\mu_{\omega}) \approx \frac{1}{N} \sum_{i=1}^N \nabla_a Q(s, a|\theta) \Big|_{s=s_i, a=\mu_{\omega}(s)} \nabla_{\omega} \mu(s|\omega) \Big|_{s_i},$$

where N is the mini-batch size from the replay buffer [10]. The target actor and critic networks in DDPG are updated via exponential moving averages of the behavior networks' parameters:

$$\hat{\omega} \leftarrow \tau \omega + (1 - \tau) \hat{\omega}, \quad \hat{\theta} \leftarrow \tau \theta + (1 - \tau) \hat{\theta},$$

where $\tau \in (0, 1)$ controls the update rate for greater stability. Traditional RL methods, including DDPG, often rely on fully connected feed-forward neural networks (FFNNs) for making an action, which do not capture the topological structure of communication networks. While some approaches use convolutional neural networks (CNNs) to capture spatial relationships, CNNs are based on Euclidean structures and struggle with the irregular, non-Euclidean topology of communication networks. Furthermore, RL environments modeled as Markov Decision Processes (MDPs) assume the Markov property, which real-world internet traffic often violates due to non-stationarities (non-Markovian properties). Therefore, we employ Gated Recurrent Units (GRUs) with a temporal attention mechanism and Graph Attention Networks (GATs) to address these challenges as follows.

III. GATED RECURRENT UNITS

Firstly, Gated Recurrent Units (GRUs) are a type of Recurrent Neural Network (RNN) designed for processing sequential data (e.g., internet traffic sequences). GRUs maintain temporal dependencies via a hidden state mechanism [13], where hidden states $h^t \in \mathbb{R}^d$ act as memory, storing information from previous time steps. The hidden states are dynamically updated to retain or discard information, ensuring that only relevant information is stored and utilized, with d representing the hidden state dimension. These hidden states h^t at each time step t are updated using the current input x_t and the previous hidden state h_{t-1} as follows:

$$h^t = f(Wx^t + Uh^{t-1} + b), \quad (2)$$

where W and U are weight matrices, b is the bias, and f is typically \tanh or ReLU for non-linearity. The input to an RNN is a time series matrix $X \in \mathbb{R}^{T \times F}$, where $\{x^1, x^2, \dots, x^T\}$ and each $x^t \in \mathbb{R}^F$ represents system features at time t . Here, T is the window size, and F is the number of features. GRUs further improve conventional RNNs by addressing the vanishing gradient problem [14] with two gates, namely the update gate z^t and reset gate r^t , which control how much past information is retained as follows:

$$z^t = \sigma(W^z x^t + U^z h^{t-1}), \quad r^t = \sigma(W^r x^t + U^r h^{t-1}), \quad (3)$$

where W^z , W^r , U^z , and U^r are learnable weights, and σ is the sigmoid function. A candidate hidden state \tilde{h}^t is computed as

$$\tilde{h}^t = \tanh(Wx^t + r^t \odot Uh^{t-1}), \quad (4)$$

where the reset gate r^t selectively controls how much of h^{t-1} contributes to h^t . The final update of the hidden state h^t combines the past and candidate hidden states:

$$h^t = z^t \odot h^{t-1} + (1 - z^t) \odot \tilde{h}^t. \quad (5)$$

As a result, the output of GRU is a sequence of hidden states:

$$H = \{h^1, h^2, \dots, h^T\} \in \mathbb{R}^{T \times d}. \quad (6)$$

A. Temporal Attention Mechanism

In GRUs, information flows sequentially, making it challenging to retain distant past information. A temporal-attention mechanism helps by focusing on specific past time steps using attention weights computed via a query-key mechanism. This mechanism involves three vectors: *query* Q , *key* K , and *value* V . The query Q represents what the current time step seeks from past steps, while K assesses the relevance of each past time step. The value vectors V hold the actual information. Attention scores are computed as the similarity between Q and K , normalized with softmax and used to weight V . The weighted sum (also called context vector) aggregates relevant information to guide the current hidden state to focus on critical information in the sequence. Mathematically, Q , K , and V are obtained by applying parameter matrices $W_Q \in \mathbb{R}^{d \times d_q}$, $W_K \in \mathbb{R}^{d \times d_k}$, and $W_V \in \mathbb{R}^{d \times d_v}$ to the GRU-generated hidden states H :

$$Q = W_Q H, \quad K = W_K H, \quad V = W_V H,$$

where $Q \in \mathbb{R}^{T \times d_q}$, $K \in \mathbb{R}^{T \times d_k}$, and $V \in \mathbb{R}^{T \times d_v}$. The attention weights α_{ij} for each past step j at time i are:

$$\alpha_{ij} = \frac{\exp(k_j^T \cdot q_i)}{\sum_{j'=1}^i \exp(k_{j'}^T \cdot q_i)} \quad \text{for } j \leq i,$$

With normalization via softmax. Then, the context vector h^a at time t is given by

$$h_t^a = \sum_{j=1}^t \alpha_{tj} \cdot v_j.$$

The context vector for all time steps is $H^a = [h_1^a, h_2^a, \dots, h_T^a] \in \mathbb{R}^{T \times d_v}$. Finally, the Hadamard product (element-wise multiplication) of H and H^a , followed by a linear transformation with $W_A \in \mathbb{R}^{d' \times d}$, yields:

$$H^A = W_A (H \odot H^a) \in \mathbb{R}^{T \times d'}. \quad (7)$$

This scales each hidden state feature based on the attention mechanism, producing H^A as the final output [24].

IV. GRAPH ATTENTION NETWORKS

Next, we model the topology of communication networks using graphs, a natural representation of non-Euclidean structured data. A graph is defined as $G = (V, E)$, where V represents nodes (e.g., routers) and E represents edges (communication links). The adjacency matrix A captures the graph structure, where $A_{ij} = 1$ if nodes i and j are connected, otherwise $A_{ij} = 0$. However, graphs are static and need adaptation in dynamic traffic environments. This is achieved

through Graph Attention Networks (GATs) which enable nodes to weigh neighbors differently via spatial attention. Let v_i denote node i for $i = 1$ to N . We use a feature matrix $\mathbf{h} = \{h_1, h_2, \dots, h_N\} \in \mathbb{R}^{N \times K}$, where $h_i \in \mathbb{R}^K$ represents node i 's features. Each feature vector is linearly transformed into a higher dimension K' using a shared weight matrix $\mathbf{W} \in \mathbb{R}^{K' \times K}$ to capture more complex patterns. To capture dependencies between nodes, we concatenate each node pair's features h_I and h_j into \tilde{h}_{ij} and apply an attention function $a : \mathbb{R}^{2K} \rightarrow \mathbb{R}$, parameterized by a weight vector $a \in \mathbb{R}^{2K}$ and LeakyReLU activation:

$$e_{ij} = \text{LeakyReLU}(a^T [\mathbf{W}h_i \parallel \mathbf{W}h_j]), \quad (8)$$

where e_{ij} represents attention coefficients, indicating the importance node i assigns to node j . The coefficients are then normalized as:

$$\alpha_{ij} = \frac{\exp(e_{ij})}{\sum_{k \in \mathcal{N}_i} \exp(e_{ik})}, \quad (9)$$

and used for weighted aggregation of neighbors' features:

$$\hat{h}_i = \sigma \left(\sum_{j \in \mathcal{N}_i} \alpha_{ij} \mathbf{W}h_j \right), \quad (10)$$

where \hat{h}_i is then used as an updated feature vector for node i and σ is an activation function. The final GAT output is the updated feature matrix:

$$\hat{\mathbf{h}} = \{\hat{h}_1, \hat{h}_2, \dots, \hat{h}_N\} \in \mathbb{R}^{N \times F}. \quad (11)$$

The overall agent architecture that employs the GRU, temporal attention, and GAT is presented in Fig. 2. We will then introduce the communication network environment and how the agent interacts with it in the following sections.

V. APPLICATION OF STRL TO NETWORK ROUTING

A. Experiment Setting

Our experiment uses the NSFNet topology, established by the National Science Foundation (NSF) during the early Internet era [25]. It includes 14 nodes and 21 communication links. We use $G = (V, E)$ to denote the graph, where:

$$V = \{\text{CO, CA, IL, \dots, GA, NY, NJ}\}$$

denotes nodes using state abbreviations, and

$$E = \{(\text{CO, CA}), (\text{CO, TX}), \dots, (\text{NJ, GA})\}$$

represents edges. To use dataset that reflect the characteristics of modern Internet data centers (IDCs), we collected the average CPU utilization rate across 4000 machines in 8 days from a real-production cluster trace published by Alibaba Group. We performed an autocorrelation analysis on the collected time series of CPU utilization rate and found temporal dependencies in its hourly data as shown in Fig. 1. Specifically, the x-axis is the time lag (hour), ranging from 1 to 48, while the y-axis is the correlation coefficient. The shaded area is a confidence interval of 95% under the null hypothesis of zero correlation. These correlation coefficients show oscillating patterns in 48 lags with statistically significant correlations in lags 1,

2, 3, 23, 24, and 25. These temporal dependencies suggest non-stationarity, which violates the Markov property. In the following section, we explain how we model these temporal dependencies in our simulated system.

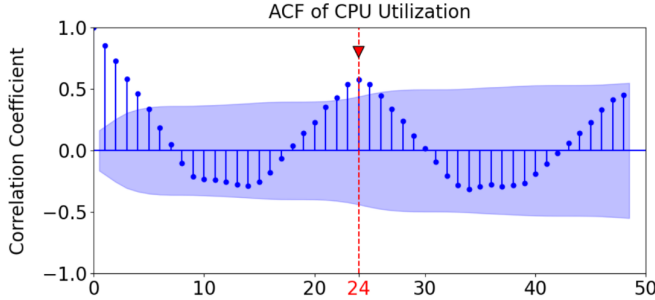


Fig. 1: Autocorrelation Function (ACF) of CPU Utilization Rate over 8 days with Hourly Time Lag

B. System Model

We link the CPU utilization rate $\rho_{\text{cpu}}(t)$ to the packet arrival rate $\lambda(t)$ through the utilization law in Eq. 12. $\rho_{\text{cpu}}(t)$ is proportional to $\lambda(t)$ (i.e., the number of packets arriving per hour), scaled by a constant C :

$$\rho_{\text{cpu}}(t) = \lambda(t) \cdot C. \quad (12)$$

Thus we can recover the temporal dependencies observed in $\rho_{\text{cpu}}(t)$ through $\lambda(t)$, and inject $\lambda(t)$ into the communication network (i.e., NSFnets). We call $\lambda(t)$ the network traffic and packets interchangeably. Each node i receives a continuous stream of traffic and processes it at a rate μ_i (i.e., the number of packets being processed per second). The processing time at each node is then determined as:

$$\frac{\lambda(t)}{\mu_i}.$$

If the node is busy, the incoming traffic is temporarily stored in the node's buffer. The processing rates μ_i are carefully set to present realistic network dynamics: rates are neither too slow (which could cause traffic to become stuck at a node) nor too fast (which could eliminate meaningful buffer delays required for optimization). Each node will next forward the packets to an outgoing link. If the link is busy, they are queued in the link's buffer. Each link then determines the transmission time $T(t)$ based on the total bandwidth demand for incoming traffic $R(t)$ and its own capacity B :

$$T(t) = \frac{R(t)}{B}, \quad R(t) = \lambda(t) \cdot L.$$

$R(t)$ is calculated as the product of the average packet size L and the number of incoming packets. L is set to 64 kb, and B is set to 1 Gbps to match realistic settings [26]. Then, each link forwards packets to the connected node and repeats the same processing as described. Note that the time interval between successive traffic arrivals is set to one hour to align with the hourly CPU utilization rate that was observed for temporal dependencies in Section V-A.

This system is used to train the agent as follows. First, we begin with a warm-up phase, where traffic is injected into all possible node pairs, with the forwarding path selected randomly for every arrival of the packet. This warm-up continues until 8 days of traffic $\lambda(t)$ are exhausted. Then we start the training phase. In this phase, the path of only one particular pair of nodes is intervened by the agent, while other pairs continue receiving traffic with random path selection. The agent needs to receive information (i.e., state) from all nodes, and then makes a path selection (i.e., action) for forwarding the incoming packet. At the end of each hour, the agent collects feedback (i.e., the reward) based on the system's performance. This feedback is used to adjust the agent's actions for routing future incoming traffic. In the next section, we formally define the state, action, and reward to understand the agent's decision-making mechanism.

C. MDP Framework

The state S is defined as a three-dimensional tensor $S \in \mathbb{R}^{24 \times 14 \times 5}$, where the dimensions represent a 24-hour time window, 14 nodes in the network, and five features for each node. The five features include one value for the node delay (average time difference between when packets exit the node and when they enter its buffer) and up to four values for packet delays on each of its outgoing links. As different nodes have different number of outgoing links (i.e., 4) and apply padding for nodes with fewer outgoing links to standardize the representation. Thus, for a node i at time t , the state is

$$S(t, i, :) = [\text{node delay}, \text{link delay 1}, \dots, \text{link delay 4}],$$

The action is a vector $A \in \mathbb{R}^{14}$, where each element $A(i)$ represents the efficiency score of node i , $i \in \{1, 2, \dots, 14\}$. These efficiency scores quantify the relative feasibility for the agent to route traffic through each node in the network. A higher efficiency score for a node indicates that it is more favorable for routing traffic, either due to lower expected delays or higher throughput capabilities. The reward function R is defined as the ratio of system throughput (η) to system delay (d). Here, η represents the system throughput, calculated as the ratio of the number of packets exiting the network to the number of packets entering it. The system delay, d , is defined as the average time difference between a packet's entry and exit from the network. The reward function therefore captures the trade-off between efficient traffic processing and delay minimization within the network. Next, we describe how agent utilizes state S to take an action A and utilizes reward R to update itself, with an overall architecture given in Fig. 2

D. Apply the Proposed STRL Algorithm

The agent processes the state $S \in \mathbb{R}^{24 \times 14 \times 5}$ using a GRU, generating hidden states $H = (h^1, \dots, h^{24}) \in \mathbb{R}^{24 \times 70}$ with a latent dimension of 70. A ReLU activation is applied to ensure non-negative hidden values, followed by a temporal attention mechanism producing $H^A \in \mathbb{R}^{24 \times 70}$. This is passed through a GAT layer to arrive at a spatial attention-weighted vector

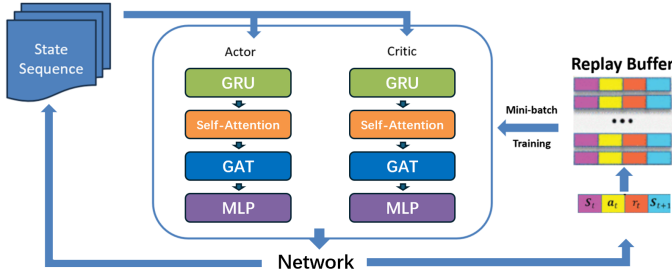


Fig. 2: STRL Architecture for Solving NSFNet Topology

$(\hat{h}_1, \dots, \hat{h}_{14})$ for each node, which is processed by a multi-layer perceptron (MLP) to generate efficiency scores. Using these scores, Dijkstra's algorithm selects the top 10 paths based on the highest cumulative feasibility scores. Rewards are calculated hourly, and experiences (state, action, reward) are stored in a replay buffer. A batch of 32 experiences is sampled per hour to compute the loss (Eq. 1), updating parameters via Bellman equations and policy gradients (Section II-B). The agent has trained over 500 episodes, each with 100 time steps, with the performance compared against baselines in the next section.

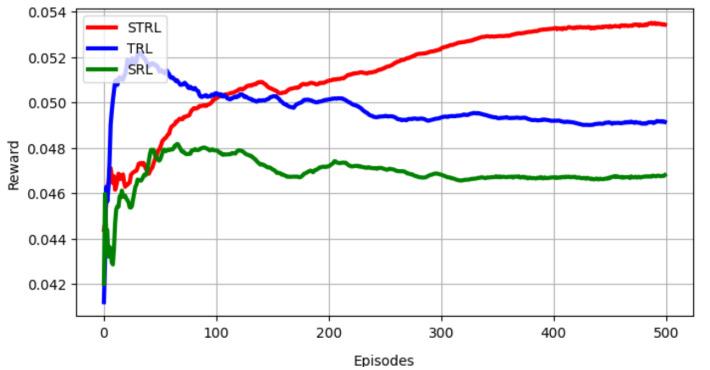
VI. PERFORMANCE EVALUATION

A. Results and Analysis

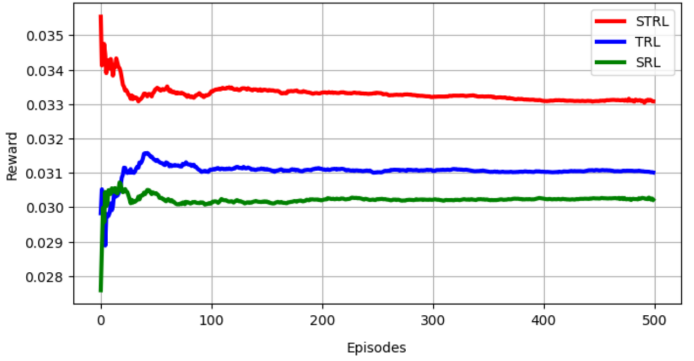
We evaluate the reward curve of STRL against two baseline models: Temporal RL (TRL) and Spatial RL (SRL). TRL only employs one GRU layer for capturing temporal information. SRL uses only one GAT layer to learn only spatial information. Fig. 3a shows that STRL achieves higher rewards, outperforming TRL by 9.18% and SRL by 14.43%.

To addition to the normal network topology, we also test the performances of the routing techniques for a modified topology by adding links between nodes ('CO', 'GA') and ('NE', 'GA'). The addition of these links creates new routing challenges, which simulate real-world scenarios when network configurations change. As shown in Fig. 3b, STRL maintains a higher reward than the two baselines. Therefore, STRL is more robust and can generalize better to unforeseen topology changes.

Finally, to evaluate STRL's ability to capture temporal patterns for the normal network topology, we analyze the GRU hidden states $H = (h^1, \dots, h^{24}) \in \mathbb{R}^{24 \times 70}$, where each time step has 70 hidden state units, which each unit encodes a distinct learned pattern (Fig. 4). These hidden states H are then passed through a ReLU activation, where negative values in H are deactivated (set to 0), and only positive values can influence subsequent processing. Different hidden units capture different temporal patterns. For example, some units (e.g., 0th, 42th, 58th) are more active at early time steps (hours), therefore capturing short-term dependencies, other units (e.g., 2th, 15th, 70th) show stronger activation at later time steps, capturing longer-term dependencies. These hidden units with larger positive values also indicate a stronger temporal influence for predicting their future behavior. Thus,



(a) Learning Curves for the Normal Network Topology



(b) Performance for the Modified Network Topology

Fig. 3: Reward Comparison Among STRL, TRL, and SRL

these observations have aligned with the temporal patterns from the CPU utilization rate in Fig. 1, where the traffic at earlier and later time lags have significant predictive power for its future.

VII. RELATED WORKS

Convolutional Neural Networks (CNNs) are commonly used to model spatial correlations but struggle with irregular network topologies due to their grid-like structure assumptions [16], [17]. Graph Neural Networks (GNNs) have been used for routing optimization in Software-Defined Networks (SDNs), focusing primarily on spatial information with limited temporal integration [18]–[20]. While [21] applies GAT with time series link loads to capture temporal aspects, it focuses on link-level congestion prediction rather than routing optimization. For temporal modeling, frameworks like the periodic Markov Decision Process (MDP) capture periodic patterns and leverage Proximal Policy Optimization (PPO) for phase-based policy learning [22], [23]. Although effective for periodic trends, pMDP may struggle with complex temporal variations. Integrating GNNs with temporal reinforcement learning could address these challenges by capturing both spatial and temporal dynamics, an area still underexplored.

VIII. CONCLUSION

This paper proposes a spatial-temporal reinforcement learning approach for packet routing with non-Markovian traffic.

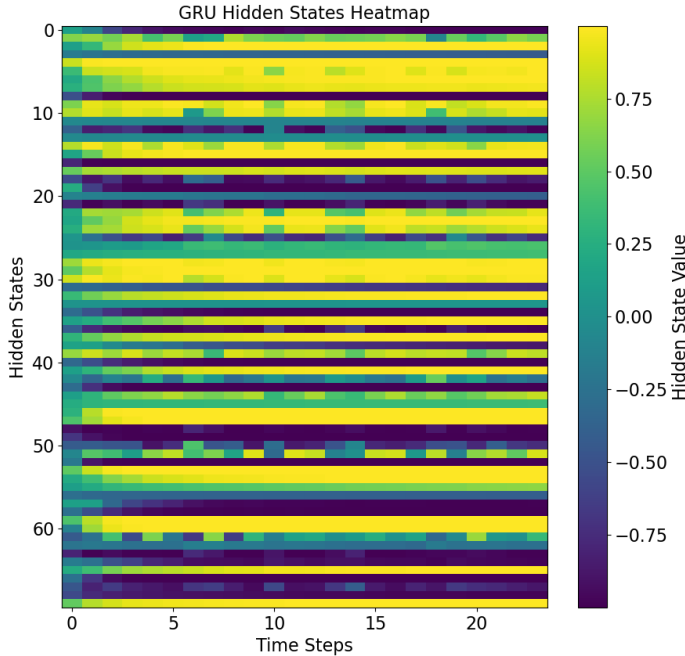


Fig. 4: GRU Hidden State Heatmap

The proposed method outperforms two RL baselines and demonstrates strong robustness to topology changes. However, several improvements can be made. Although a self-attention mechanism is employed, future work could investigate transformer-based models [24] to better capture long-range dependencies in sequential traffic data. Additionally, in large-scale networks, a distributed approach can be considered to address the scalability issues.

REFERENCES

- [1] J. Chen, et al., "Use Coupled LSTM Networks to Solve Constrained Optimization Problems," in *IEEE Trans. Cognitive Commun. and Networking*, vol. 9, no. 2, pp. 304-316, 2022.
- [2] H. Xu and W. Wang, "Machine learning approaches for network routing," *IEEE Trans. Netw.*, vol. 28, no. 5, pp. 2528–2539, 2020.
- [3] Y. Sun, et al., "Deep Q-learning for SDN routing," *IEEE Access*, vol. 7, pp. 93577–93584, 2019.
- [4] Q. Zhang, et al., "An SDN-based traffic engineering approach using deep reinforcement learning," *IEEE Internet Things J.*, vol. 6, no. 3, pp. 4925–4936, 2019.
- [5] T. Lillicrap, et al., "Continuous control with deep reinforcement learning," *arXiv preprint arXiv:1509.02971*, 2015.
- [6] M. Papagiannaki, et al., "Non-Markovian nature of internet traffic," *IEEE/ACM Trans. Netw.*, vol. 16, no. 5, pp. 1054–1067, 2008.
- [7] S. Chen and L. Li, "Periodic MDPs for diurnal network patterns," in *Proc. ACM CoNEXT*, 2023.
- [8] V. Mnih, et al., "Asynchronous methods for deep reinforcement learning," in *Proc. ICML*, 2016.
- [9] R. J. Williams, "Simple statistical gradient-following algorithms for connectionist reinforcement learning," *Mach. Learn.*, vol. 8, no. 3–4, pp. 229–256, 1992.
- [10] T. Lillicrap, et al., "Continuous control with deep reinforcement learning," *arXiv preprint arXiv:1509.02971*, 2015.
- [11] D. Silver, et al., "Deterministic policy gradient algorithms," in *Proc. ICML*, 2014.
- [12] V. Mnih, et al., "Asynchronous methods for deep reinforcement learning," in *Proc. ICML*, 2016.
- [13] K. Cho, et al., "Learning phrase representations using RNN encoder-decoder for statistical machine translation," *arXiv preprint arXiv:1406.1078*, 2014.
- [14] Y. Bengio, et al., "Learning long-term dependencies with gradient descent is difficult," *IEEE Trans. Neural Netw.*, vol. 5, no. 2, pp. 157–166, 1994.
- [15] A. Vaswani, et al., "Attention is all you need," in *Proc. NIPS*, 2017, pp. 5998–6008.
- [16] H. Chen, et al., "Dynamic convolutional models for structured data," in *Proc. IEEE Big Data*, 2020.
- [17] T. Anderson, et al., "Limitations of CNNs for non-Euclidean data," *IEEE Trans. Neural Netw. Learn. Syst.*, vol. 32, no. 7, pp. 3115–3128, 2021.
- [18] J. Chen, et al., "Graph neural networks in SDN routing optimization," in *Proc. IEEE INFOCOM*, 2021.
- [19] A. Kalra, et al., "Simulation-driven GNN for network optimization," in *Proc. ACM SIGCOMM*, 2021.
- [20] Y. Xu, et al., "Integrating GNNs with routing algorithms," *IEEE J. Sel. Areas Commun.*, vol. 39, no. 3, pp. 615–624, 2021.
- [21] K. Poularakis, et al., "Graph attention networks for link congestion," in *Proc. IEEE ICNP*, 2020.
- [22] S. Chen and L. Li, "Periodic MDPs with PPO for network learning," in *Proc. IEEE Int'l Conf. Netw. Protocols*, 2021.
- [23] Z. Chen, et al., "Learning Technique to Solve Periodic Markov Decision Process for Network Resource Allocation," in *Proc. IEEE MILCOM*, 2023.
- [24] A. Vaswani, et al., "Attention is all you need," in *Proc. NIPS*, 2017, pp. 5998–6008.
- [25] National Science Foundation, "The National Science Foundation Network (NSFNET): A foundation for advanced networking and the early internet," *NSF Archives*, 1985.
- [26] J. W. Doherty, "More packet loss when transmitting 64-byte frame size than 1518-byte," *Cisco Community*, Mar. 2018.